Neuro-Oncology 13(1):51–60, 2011.
doi:10.1093/neuonc/noq150
Advance Access publication December 1, 2010

Dynamic magnetic resonance imaging assessment of vascular targeting agent effects in rat intracerebral tumor models

Leslie L. Muldoon, Seymur Gahramanov, Xin Li, Deborah J. Marshall, Dale F. Kraemer, and Edward A. Neuwelt

Department of Neurology (L.L.M., S.G., E.A.N.), Department of Cell and Developmental Biology (L.L.M.), Advanced Imaging Research Center (X.L.), Department of Neurosurgery (E.A.N.), Department of Public Health and Preventive Medicine (D.F.K.), Department of Medical Informatics (D.F.K.), Department of Clinical Epidemiology (D.F.K.), Oregon Health and Science University, Portland, Oregon; Ortho Biotech Oncology R&D, Radnor, Pennsylvania (D.J.M.); Department of Pharmacy Practice, Oregon State University, Portland, Oregon (D.F.K.); Portland Veterans Administration Medical Center, Portland, Oregon (E.A.N.)

We used dynamic MRI to evaluate the effects of monoclonal antibodies targeting brain tumor vasculature. Female athymic rats with intracerebral human tumor xenografts were untreated or treated with intetumumab, targeting α_V-integrins, or bevacizumab, targeting vascular endothelial growth factor ($n = 4–6$ per group). Prior to treatment and at 1, 3, and 7 days after treatment, we performed standard MRI to assess tumor volume, dynamic susceptibility-contrast MRI with the blood-pool iron oxide nanoparticle ferumoxytol to evaluate relative cerebral blood volume (rCBV), and dynamic contrast-enhanced MRI to assess tumor vascular permeability. Tumor rCBV increased by 27 ± 13% over 7 days in untreated rats; intetumumab increased tumor rCBV by 65 ± 10%, whereas bevacizumab reduced tumor rCBV by 31 ± 10% at 7 days ($P < .001$ for group and day). Similarly, intetumumab increased brain tumor vascular permeability compared with controls at 3 and 7 days after treatment, whereas bevacizumab decreased tumor permeability within 24 hours ($P = .0004$ for group, $P = .0081$ for day). All tumors grew over the 7-day assessment period, but bevacizumab slowed the increase in tumor volume on MRI. We conclude that the vascular targeting agents intetumumab and bevacizumab had diametrically opposite effects on dynamic MRI of tumor vasculature in rat brain tumor models. Targeting α_V-integrins increased tumor vascular permeability and blood volume, whereas bevacizumab decreased both measures. These findings have implications for chemotherapy delivery and antitumor efficacy.

Keywords: bevacizumab, blood–brain barrier, dynamic susceptibility-weighted contrast-enhanced magnetic resonance imaging, intetumumab.

Central nervous system tumors induce neovascularization resulting in blood vessels that differ significantly from normal brain vasculature.[1] Agents that specifically target tumor vasculature are gaining use in brain tumor therapy.[2,3] The rationale for using vascular-targeted agents is based on the concept that normalization of tumor vasculature, pruning of aberrant vessels, and blockage of new angiogenesis will starve the tumor and improve access of cytoreductive drugs to tumor cells.[4,5] In the brain, however, vascular normalization may restore the low-permeability characteristics of the normal blood–brain barrier (BBB), resulting in decreased vascular permeability to chemotherapy.

Angiogenesis and control of BBB permeability are complex phenomena involving multiple pathways. One of the key regulators of angiogenesis is the vascular endothelial growth factor (VEGF) system, components of which are often overexpressed in brain tumors.[4,6] Bevacizumab (Avastin), a monoclonal antibody (mAb) targeting VEGF, has antitumor efficacy in animal models,[7,8] and clinically in recurrent glioblastoma.[9,10] Another approach is to target angiogenic vascular endothelial cells by blocking cell surface integrins.[11,12] The anti-α_V integrin mAb intetumumab (CNTO 95) binds cell surface proteins important

Received April 19, 2010; accepted August 13, 2010.

Corresponding Author: Edward A. Neuwelt, MD, Oregon Health and Science University, 3181 S.W. Sam Jackson Park Road, L603, Portland, OR 97239-3098 (neuwelte@ohsu.edu).

for cell–cell adhesion and angiogenesis. Intetumumab has shown efficacy in solid tumor xenograft and metastasis models[13,14] and has entered clinical trials in subjects with advanced solid tumors.[15] We hypothesized that both bevacizumab and intetumumab would alter vascular permeability in brain tumors.

New dynamic MRI techniques provide quantitative characterization of tumor vasculature in vivo. Dynamic susceptibility-weighted contrast-enhanced MRI (DSC-MRI, also referred to as perfusion-weighted imaging) can be used to assess tumor relative cerebral blood volume (rCBV), which has shown potential for determining response to therapy in human glioblastoma.[16,17] High rCBV is thought to indicate active neovascularization and viable tumor.[17–19] DSC-MRI is most accurate when a blood-pool contrast agent such as ferumoxytol iron oxide nanoparticles is used to minimize leakage artifacts.[8,20,21] Alternatively, dynamic contrast-enhanced (DCE) MRI can be used to characterize contrast leakage across the BBB and tumor vasculature with high spatial and temporal resolution. Tissue pharmacokinetic parameters derived from DCE-MRI signal-intensity time-course data offer quantitative assessment of blood vessel permeability to low molecular weight gadolinium-based contrast agents (GBCAs). DCE-MRI has been used to monitor angiogenesis[22,23] and predict therapeutic efficacy.[24] The goal of this study was to use DSC and DCE dynamic MRI to assess the effects of vascular targeting antibodies on brain tumor vascular volume and permeability.

Methods

Agents

Intetumumab (CNTO 95) was provided by Centocor, Inc. Ferumoxytol (Feraheme) was provided by AMAG Pharmaceuticals. Bevacizumab (Avastin, Genentech Inc.) was obtained from the Oregon Health and Science University (OHSU) pharmacy.

Cell Lines Used in These Studies

Human tumor cell lines were UW28 glioma (obtained from Dr Ali-Osman, Duke University, Durham, NC, in 1996), DAOY medulloblastoma (obtained from American Type Culture Collection), LX-1 small cell lung carcinoma (SCLC) (obtained from Mason Research Institute, Worcester, MA), and MDA-MB231BR-HER2 breast carcinoma cells expressing high levels of HER2 (obtained from Dr Pat Steeg, National Cancer Institute, in 2005). Cells were cultured in RPMI-1640 (LX-1 cells) or Dulbecco's modified Eagle's medium (all other cell lines) supplemented with 10% fetal bovine serum and antibiotics.

Animal Models

The care and use of animals were approved by the Institutional Animal Care and Use Committee and were supervised by the OHSU Department of Comparative Medicine. Female athymic nude rats (rnu/rnu, 200–240 g, from the OHSU BBB Program in-house colony) were anesthetized with i.p. ketamine (60 mg/kg) and i.p. diazepam (7.5 mg/kg). Animals received $1.2–1.5 \times 10^6$ of more than 90% viable cells in a volume of 15 μL, stereotactically injected in the right caudate nucleus (vertical, bregma 5 mm; lateral, bregma 3 mm). The needle was initially advanced to a depth of 6.5 mm and then withdrawn to a depth of 5 mm to limit reflux up the needle track. Animals were sacrificed if they showed severe clinical symptoms or >20% weight loss.

In the pilot study, rats with all 4 tumor types (3 rats per tumor type) underwent baseline dynamic MRI at 12 T, then received intetumumab i.v.; the initial 4 rats in the study received 10 mg/kg, and all other animals received 30 mg/kg. Follow-up MRI was done 48 hours after treatment. In the treatment study, rats with LX-1 SCLC intracerebral xenografts were randomized to 3 treatment groups—Group 1, untreated control; Group 2, intetumumab 30 mg/kg i.v.; and Group 3, bevacizumab 45 mg/kg i.v. ($n = 4–6$ per group). The goal was to have $n = 4$ rats at the final imaging time point; 2 rats in the intetumumab group and 1 rat in the control group died early and were replaced. Rats were imaged prior to treatment at 10 days after tumor implantation and at 1, 3, and 7 days after treatment. Initial rats were also scanned at 2 hours after treatment, but we found signal contamination from the pretreatment scan, so the 2-hour point was discontinued.

Magnetic Resonance Imaging

Animals were anesthetized using i.p. medetomidine (0.6 mg/kg, Pfizer Animal Health) and ketamine (15 mg/kg) for MRI using the 12-T MRI scanner (Bruker) with a custom rat head coil. Throughout the MR scans, animals were wrapped in a warm-water blanket, and oxygen saturation and heart rate were monitored. High-resolution anatomical T2-weighted scans (repetition time [TR]/echo time [TE] 5500/30 ms, flip angle 180°, slice thickness 1 mm, field of vision [FOV] 3.2×3.2 cm^2, matrix 384×384) were performed in both the coronal and axial planes for accurate planning of the DSC and the DCE studies. The DSC gradient echo-imaging parameters were: TR/TE 9.7/4.0 ms, flip angle 5°, slice thickness 1.4 mm, with a 0.6 s/image time resolution, and 280×200 μm spatial resolution. During rapid single-slice coronal T2*-weighted image acquisition, ferumoxytol (1.8 mg of Fe in 60 mL, 7–9 mg/kg) was infused at 3 ml/min via a tail vein catheter. The DCE permeability measurement was performed 5–15 minutes after DSC-MRI, using gadodiamide bolus (60 μL of 250 mM Omniscan, GE Healthcare) administered at a 1-mL/min flow rate during rapid repeated single-slice T1-weighted image acquisition. The DCE single-slice T1-weighted gradient echo-acquisition parameters were: TR 25.0 ms, TE 1.7 ms, flip angle 20°, slice thickness 1.0 mm, with a

1.6 s/image time resolution, and 400 × 400 μm spatial resolution. After the dynamic MRI, postcontrast anatomical T1-weighted scans were obtained in both the coronal and axial planes (TR/TE 160/1.4 ms, flip angle 40°, slice thickness 1 mm, FOV 3.2 × 3.2 cm^2, matrix 128 × 128) for tumor enhancement visualization. Following the MRI, the medetomidine was reversed using 1 mg atipamezole (Antisedan, Pfizer Animal Health).

Perfusion parametric maps were processed using Lupe software. At each time point, rCBV was calculated as a ratio of the blood volume in a region of interest (ROI) in tumor compared with normal appearing (contralateral) brain tissue. The same ROI was analyzed between time points, normalized to the highest rCBV in the pretreatment parametric maps. Permeability was calculated from the DCE-MRI time-intensity curves, in the same ROI used for rCBV measurement. Permeability is defined as the ratio of the maximum signal intensity to the time-to-peak enhancement, encompassing both K^{trans} and v_e. Tumor volume was measured based on the T2 signal changes and postcontrast T1 signal hyperintensity.

Histology

Immediately after the 7-day MRI, the rat brains were excised and fixed in 10% buffered formalin for vibratome sectioning at 100 μm in the coronal plane. For tumor volumetrics, every sixth brain section was stained with hematoxylin and then imaged at 30 μm pixel diameter resolution on an Epson 1640XL flatbed scanner using Adobe Photoshop software. Tumor volumes were assessed using National Institutes of Health ImageJ software as we have validated previously.[7,8] Immunohistochemistry was performed by incubating the brain slices with proper dilutions (1:50–1:2000) of primary antibodies and appropriate biotinylated secondary antibody and visualized with the Vectastain ABC kit (Vector Laboratories) using diaminobenzidine. Mouse anti-VEGF-R1 (sc-65442) was purchased from Santa Cruz Biotechnology, Inc., and mouse anti-CD68 (clone ED1) was from AbD Serotec. Microscopy was imaged with an Axiocam digital camera mounted on a Zeiss Axioplan microscope (Carl Zeiss Co.).

Data Analysis and Statistical Considerations

Repeated-measures analysis of variance (ANOVA) models were fit to these data. For MRI tumor volumes, the ANOVA model includes imaging measure (T1 vs T2), group (bevacizumab, intetumumab, and control), and day (1, 3, 7). Since all values were normalized to the baseline on day 0, the day 0 data were excluded. For rCBV and permeability, the ANOVA model includes only group and day. For each ANOVA model, several different covariance structures (compound symmetry, first-order autoregressive, Huynh–Feldt, first-order Toeplitz, and unstructured) were fit to the data, and the one that provided the best fit (as assessed by the corrected Akaike Information Criteria) was used to fit the final model. Least-square means were estimated for significant effects ($P < .05$), and the differences between pairs of means or pairs of interactions were assessed using a Tukey correction to account for multiple comparisons. All tests were run using SAS Version 9.2 for Windows. No power calculations were made a priori or post hoc.

Results

Effect of Intetumumab in Multiple Brain Tumor Models

In a pilot study, the effects of intetumumab were assessed in rats with large, well-vascularized intracerebral tumors, including 2 primary human brain tumor models (UW28 glioma and DAOY medulloblastoma) and 2 metastatic human brain tumor models (LX-1 SCLC and MDA-MB231BR-HER2 breast carcinoma; $n = 3$ per tumor type). Rats underwent baseline dynamic MRI at 12 T when tumors were large and well vascularized, then received intetumumab i.v. at 10 or 30 mg/kg in an effort to maximize vascular effects. Follow-up MRI was done 48 hours after treatment to match the maximal time for bevacizumab vascular effects in a previous study.[8]

There were minimal effects of intetumumab on MRI at the 2-day time point comparing pretreatement scans with scans taken 48 hours after treatment in the 4 tumor types tested (Fig. 1); these effects did not mimic our previous studies with bevacizumab.[7,8] Each tumor increased in size during the 2-day treatment period. The corresponding parametric maps from the DSC-MRI with ferumoxytol did not show significant changes in rCBV in tumors at the 2-day time point (data not shown). T1-weighted scans with GBCA before and after intetumumab treatment showed a general overall increase in signal intensity throughout the tumor, suggestive of minimally increased tumor permeability (data not shown). It was not possible to determine from this pilot study if the modest effects on blood volume and permeability were due to intetumumab or could be attributed merely to tumor growth.

Changes in rCBV

The second study was a detailed evaluation of vascular changes over time in a single-tumor model. The model chosen was the LX-1 SCLC intracerebral xenograft because of the well-characterized consistent growth of these brain tumors.[25,26] The rats were randomized to untreated controls, intetumumab 30 mg/kg i.v., or bevacizumab 45 mg/kg i.v. Rats underwent dynamic MRI immediately prior to treatment, and then 24 hours, 3 days, and 7 days after treatment.

Figure 2A shows T2-weighted images collected before (top) and 7 days after treatment (bottom) in the 3 treatment groups. The corresponding parametric maps from the DSC-MRI show areas of high blood volume. DSC-MRI with ferumoxytol was used to assess rCBV in

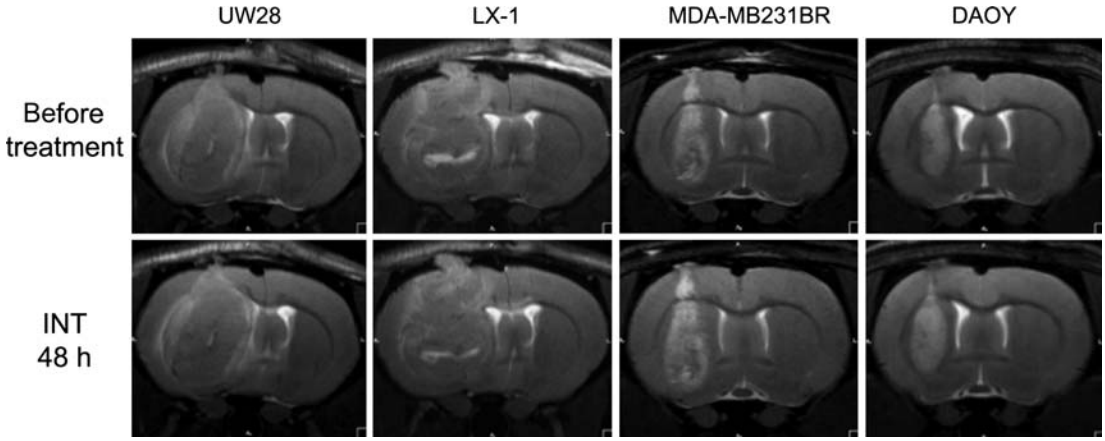

Fig. 1. MRI of tumor growth in 4 intracerebral human tumor models. Rats with intracerebral UW28 glioma, LX-1 SCLC, MDA-MB231BR-HER2 breast carcinoma, and DAOY medulloblastoma tumors underwent T2-weighted MRI before (top row) and 48 hours after (bottom row) i.v. administration of intetumumab (30 mg/kg).

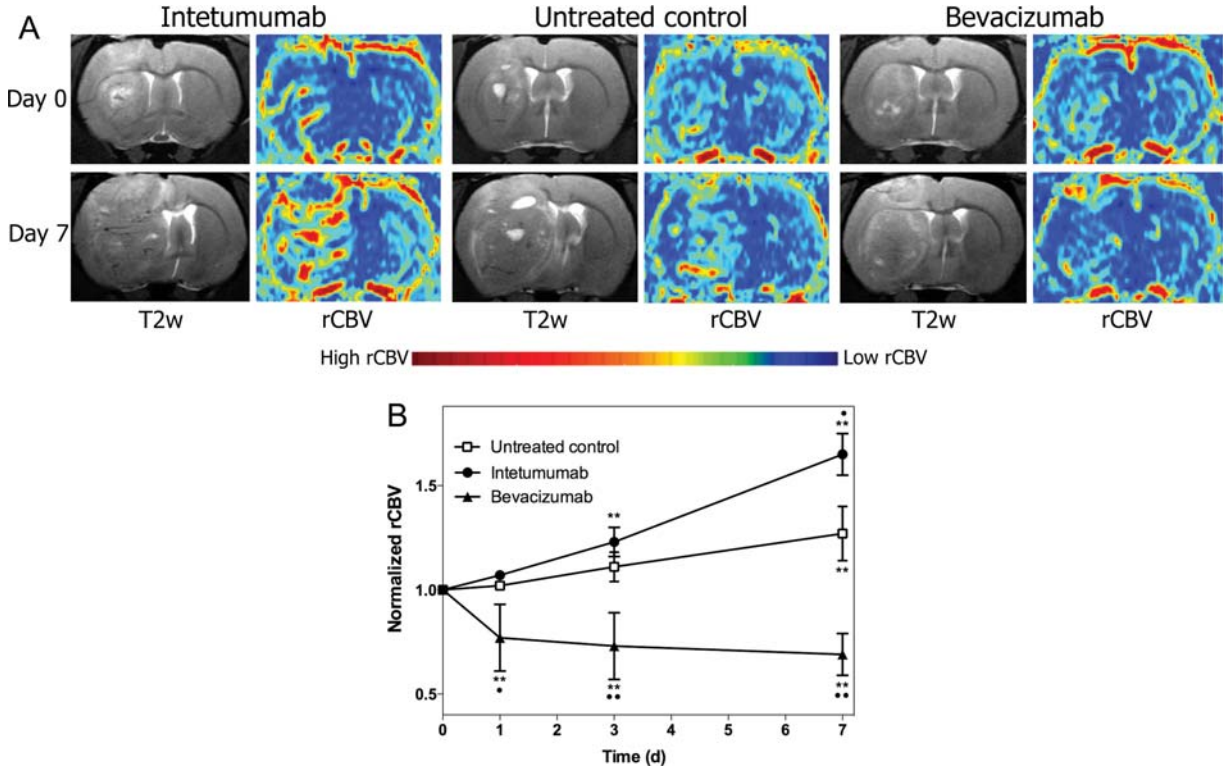

Fig. 2. Effect of intetumumab and bevacizumab on tumor rCBV. Rats with intracerebral LX-1 SCLC xenografts were randomized to no treatment, intetumumab (30 mg/kg i.v.), or bevacizumab (45 mg/kg i.v.) and underwent serial DSC-MRI with ferumoxytol. (A) T2-weighted MRI and false-color rCBV parametric maps are shown prior to treatment (day 0, top row) and 7 days (bottom row) after each treatment. Areas of high blood volume (red) are prominent after intetumumab, whereas low blood volume (blue) is found after bevacizumab treatment. (B) Blood volume determined from DSC-MRI at each time point was normalized to the pretreatment rCBV values. Mean and standard deviation are indicated for $n = 4–6$ rats per time point, showing increased rCBV after intetumumab and decreased rCBV after bevacizumab. In comparison with baseline, $^{**}P < .001$; in comparison with control at each time point, $^{\bullet}P < .05$ and $^{\bullet\bullet}P < .001$.

all animals (Fig. 2B). Untreated control rats demonstrated a $27 \pm 13\%$ increase in rCBV from baseline at 7 days ($P < .0001$). Intetumumab increased tumor blood volume from baseline at 3 days ($23 \pm 7\%$, $P < .0001$) and 7 days ($65 \pm 10\%$, $P < .0001$) after treatment and was significantly different from untreated controls ($P = .0026$). In contrast, bevacizumab significantly decreased blood volume from baseline values at every time point,

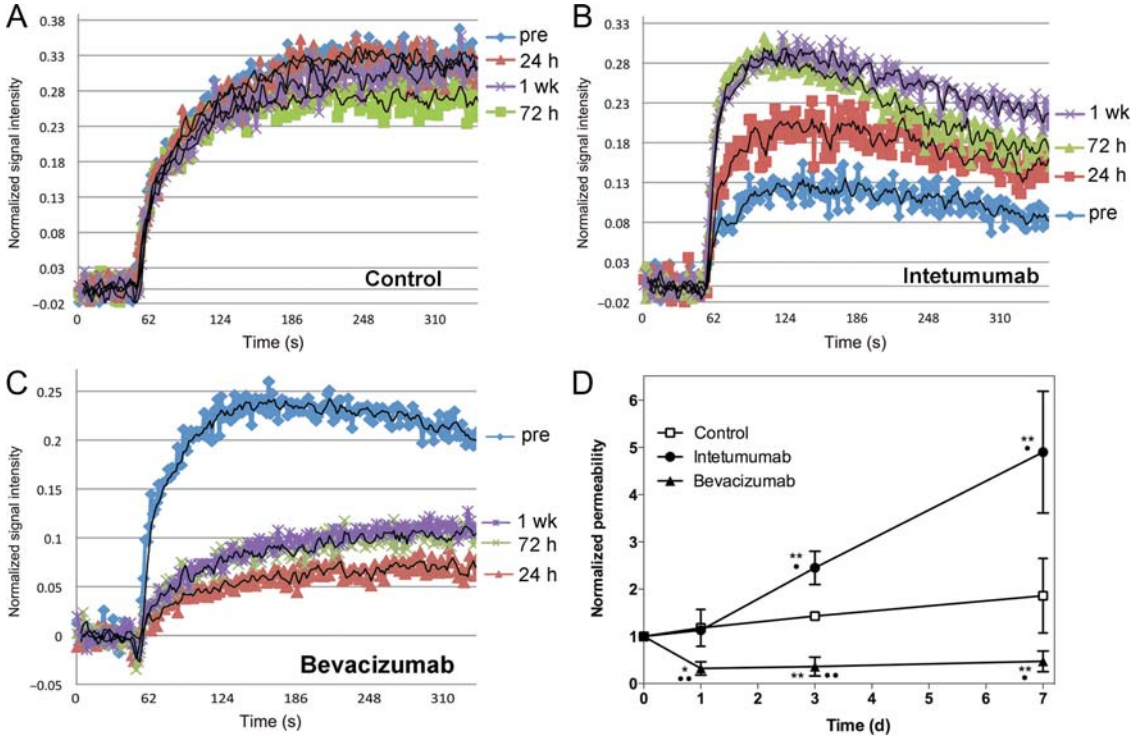

Fig. 3. Effect of intetumumab and bevacizumab on vascular permeability. Rats with intracerebral LX-1 SCLC xenografts underwent serial DCE-MRI with GBCA. Changes in normalized signal intensity are shown in (A) control untreated rat; (B) rat treated with intetumumab 30 mg/kg i.v.; (C) rat treated with bevacizumab 45 mg/kg i.v. Scans were obtained before treatment (pre; blue) and 24 hours (red), 72 hours (green), and 1 week (purple) after treatment. (D) The time-intensity mean and the standard error are indicated for $n = 4–6$ rats per time point, showing increased permeability after intetumumab and decreased permeability after bevacizumab. In comparison with baseline, $*P < .05$ and $**P < .001$; in comparison with control at each time point, $^{\bullet}P < .05$ and $^{\bullet\bullet}P < .001$.

with a maximum $31 \pm 10\%$ decrease in rCBV at 7 days ($P < .0001$ compared with control). Repeated-measures ANOVA indicated that all treatment groups were significantly different by group, day, and the interaction of group and day ($P < .0001$ for each effect).

Changes in Vascular Permeability

Brain tumor vascular permeability was assessed by DCE-MRI. The time-intensity curves derived from the DCE-MRI remain relatively stable over time in an untreated control intracerebral LX-1 tumor (Fig. 3A), showing that vascular permeability increases only minimally as the tumor grows. In intetumumab-treated tumors (Fig. 3B), normalized DCE signal intensity increased at each time point, with the maximal effect observed at 1 week after treatment. The time-to-peak intensity decreased, particularly at the 3- and 7-day time points, indicating that the rate of GBCA extravasation into tumor was increased after intetumumab treatment. In contrast, bevacizumab decreased GBCA signal intensity and prolonged the time-to-peak enhancement at all time points after treatment (Fig. 3C), with changes noted as early as 24 hours after treatment. The time-intensity data indicate that intetumumab and bevacizumab had opposite effects on both the magnitude of GBCA leakage and time-to-peak enhancement, a surrogate for rate constant for passive diffusion across the BBB.

The ratio of maximum signal intensity to time to peak was calculated to give a single measure of permeability. Figure 3D demonstrates the time course for changes in vascular permeability in the LX-1 brain tumor model. Untreated tumors showed a nonsignificant increase in permeability over time. Treatment with intetumumab significantly increased permeability, by $145 \pm 86\%$ over baseline at 3 days and $390 \pm 260\%$ at 7 days ($P = .0091$ compared with control). In contrast, bevacizumab significantly decreased brain tumor permeability at each time point compared with baseline, ranging from a $68 \pm 14\%$ decline at 24 hours to a $53 \pm 22\%$ decrease at 7 days ($P = .0218$ compared with control). Repeated-measures ANOVA demonstrated that treatment groups differed by group ($P = .0004$), day ($P = .0081$), and the interaction of group and day ($P = .0238$).

Tumor Growth and Histology

Tumor volumes were measured on T2- and T1-weighted MRI with GBCA at each time point. Normalized changes in tumor volumes on MRI are shown in Fig. 4A and B. Repeated-measures ANOVA showed no significant effects of measure (T1- vs T2-weighted, $P = .54$) or

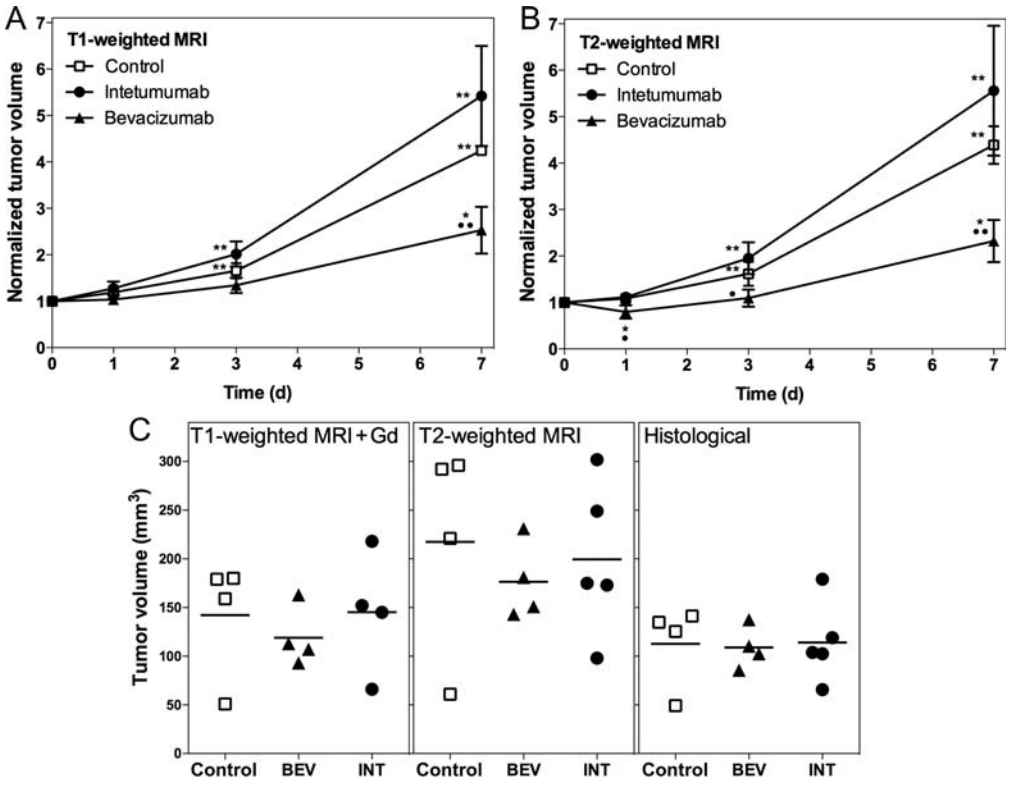

Fig. 4. Effect of vascular targeting agents on brain tumor volume. Rats with intracerebral LX-1 SCLC xenografts received intetumumab (30 mg/kg i.v.; circles) or bevacizumab (45 mg/kg i.v.; triangles), in comparison with untreated controls (squares). Normalized tumor volume changes over time were assessed on anatomical MRI scans obtained using T1-weighted with GBCA (A) or T2-weighted (B) sequences. The mean and the standard deviation are indicated for $n = 4–6$ rats per time point, showing decreased growth rate in bevacizumab-treated tumors. In comparison with baseline, $^{*}P < .05$ and $^{**}P < .001$; in comparison with control at each time point, $^{\bullet}P < .05$ and $^{\bullet\bullet}P < .001$. C shows final tumor volumes (individual animals and means) assessed on T1-weighted + GBCA MRI, T2-weighted MRI, and histological sections.

interactions between measure and group or measure and day. There are significant differences among the days ($P < .0001$) and groups ($P = .0012$) and a significant interaction between group and day ($P = .0080$). Bevacizumab-treated tumors showed $145 \pm 49\%$ increase from baseline at 7 days ($P = .0116$) and a decreased rate of volume change compared with controls ($P = .0062$). Untreated controls and tumors treated with intetumumab showed significant increases from baseline at every time point; however, these groups were not significantly different ($P = .1421$). Final actual tumor volumes are shown for histological sections in comparison with T2- and post-contrast T1-weighted MRI (Fig. 4C). Volumes were highest on T2-weighted images and lowest on histological measurements, but there were no significant differences between groups by any measure. Correlation between histological and MRI volume measurements was $r = .95$ for T1-weighted with GBCA and $r = .86$ for T2-weighted images.

Immunohistochemistry for VEGF receptor type 1 (VEGFR1) showed changes in blood vessel size and morphology in histological sections (Fig. 5A–C). Intetumumab-treated tumors showed multiple enlarged blood vessels, whereas bevacizumab-treated tumors showed minimal vessel staining. In control rats, blood vessel volume as determined by VEGFR1 staining was approximately 2.1% of tumor volume; this was increased to 3.3% after intetumumab treatment and decreased to 0.36% after bevacizumab treatment. CD68 immunohistochemistry (Fig. 5D–F) demonstrated macrophage infiltration in and around all brain tumors, irrespective of treatment. Tumor necrosis, judged by the morphology of amorphous sheets of cell debris surrounded by macrophages, was markedly increased in bevacizumab-treated tumors ($25.2 \pm 5.7\%$ of tumor volume) compared with controls ($13.8 \pm 5.6\%$ of tumor volume; $P < .05$).

Discussion

Angiogenesis is a necessary step in the growth of solid tumors and metastases, but control of tumor angiogenesis is complex.[1] The VEGF pathway has an established role in promoting tumor angiogenesis. Binding of VEGF to its receptors enhances vessel cooption by tumor cells[27] and induces endothelial cell division and capillary tube formation within and around tumors.[4] Bevacizumab sequesters and neutralizes VEGF, resulting in the inhibition of new vessel growth, regression of newly

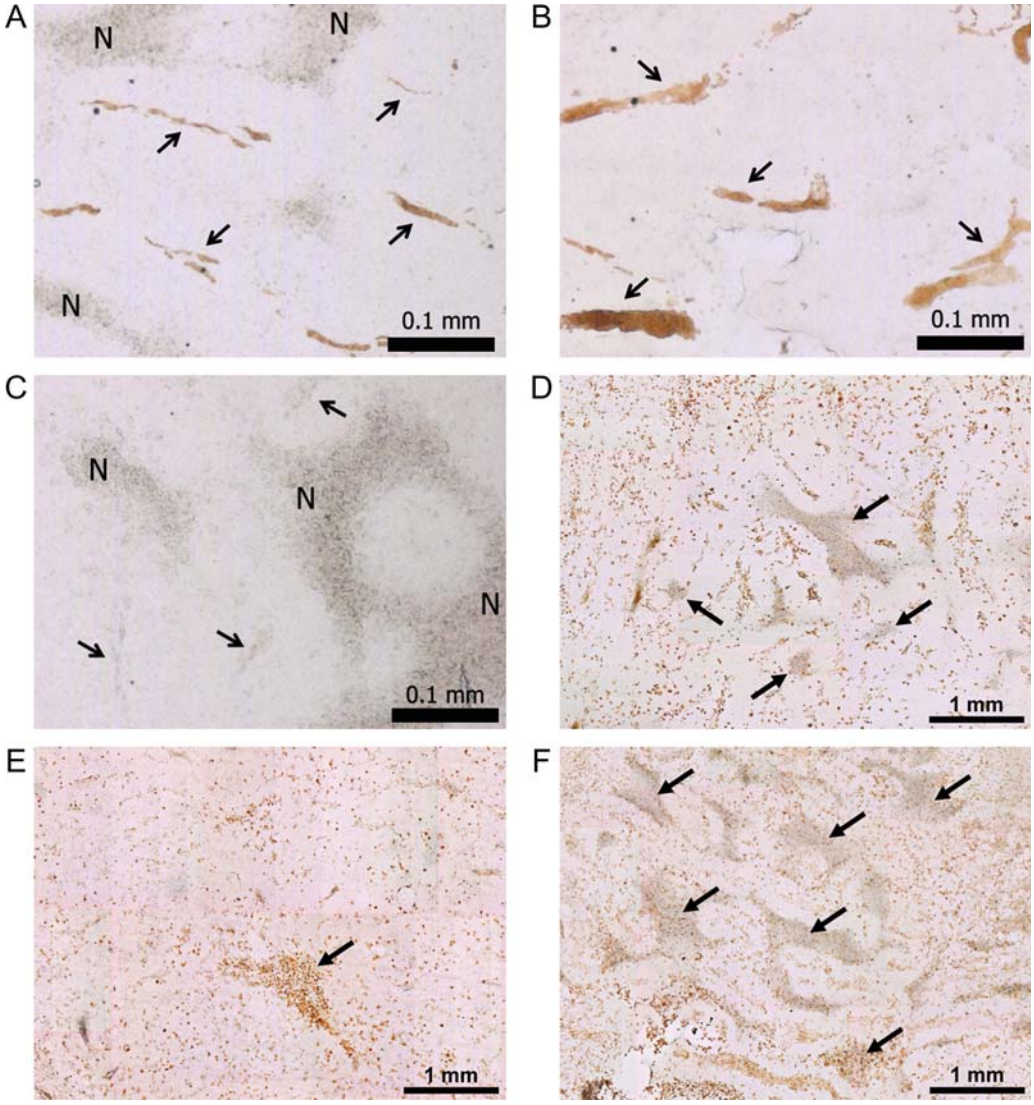

Fig. 5. Brain tumor histology. Brain sections were obtained from untreated control study rats (A and D), and rats treated with intetumumab (30 mg/kg i.v.; B and E) or bevacizumab (45 mg/kg i.v.; C and F). VEGFR1 immunohistochemistry (A–C) shows tumor blood vessels, indicated by arrows; N, areas of necrosis; bar indicates 0.1 mm. CD68 immunohistochemistry for macrophages (D–F) shows the areas of necrosis (arrows); bar indicates 1 mm.

formed vasculature, and alteration of existing tumor vessel function.[4,28]

The case for antiangiogenic activity with anti-integrins is also strong. Integrins are a family of heterodymeric membrane proteins that bind to a variety of extracellular matrix proteins that are critical to cell–cell adhesion.[11,29] Two members of the α_V-integrin group appear to be especially important for angiogenesis, but through different underlying pathways. The $\alpha_V\beta_3$ dimer promotes angiogenesis through basic fibroblast growth factor and tumor necrosis factor-α, whereas $\alpha_V\beta_5$ induces angiogenesis through VEGF and transforming growth factor-α.[14,30] Antagonists of $\alpha_V\beta_3$ integrin induce apoptosis of proliferative vascular endothelial cells, without affecting pre-existing quiescent blood vessels.[31] A pan–α_V-integrin antagonist, the cyclic pentapeptide cilengitide (EMD 121974), inhibits glioblastoma growth in animal models[32,33] and has shown promise in a phase II clinical trial.[34] Cilengitide has been shown to suppress immunostaining for CD31, a marker of neovasculature, and to inhibit angiogenesis in blood vessels by preventing the interaction of endothelial cell surface α_V-integrins with extracellular matrix ligands.[32,33] Another low-molecular-weight $\alpha_V\beta_3$ and $\alpha_V\beta_5$ inhibitor, SCH221153, inhibits angiogenesis and tumor growth in a subcutaneous melanoma model,[35] whereas Vitaxin, a mAb targeting $\alpha_V\beta_3$, has been tested in clinical trials as an antiangiogenic agent.[36] The mAb intetumumab used in the current study recognizes and blocks all α_V-integrins. It has been demonstrated to inhibit angiogenesis in several in vivo models,[14] although this report did not assess brain tumors.

It was reasonable to hypothesize that bevacizumab and intetumumab would have similar effects on brain tumor vasculature. Instead, dynamic MRI techniques demonstrated that these 2 antiangiogenic mAbs had diametrically opposite effects on brain tumor blood volume and blood vessel permeability.

Multiple investigators have reported decreases in GBCA enhancement of brain tumors after bevacizumab.[3,10] It is unclear whether many MRI changes actually represent tumor regression rather than decreased GBCA leakage.[8] A decrease in vascular permeability and perfusion in human tumors has been detected by various imaging techniques after treatment with bevacizumab as well as small-molecule VEGF receptor tyrosine kinase inhibitors.[3] Our previous studies demonstrated that bevacizumab decreased tumor vascular permeability and blood volume in glioma models,[7,8] and the current report extends this finding to lung cancer brain metastases.

DSC-MRI measurements of rCBV have been used for grading glioma malignancy and predicting survival,[17] as well as differentiating recurrent tumor from radiation necrosis[16] or pseudoprogression.[20] High blood volume indicates active neovascularization and viable tumor[17]; these measures appear to be closely correlated with microvessel density.[19] Most DSC-MRI studies have used GBCA[16,17]; our study instead used ferumoxytol for measurement of rCBV as we have reported previously.[8,37] Ferumoxytol, an ultrasmall superparamagnetic iron oxide nanoparticle approved by the Food and Drug Administration for iron replacement therapy, acts as a blood-pool agent in the short term (minutes to hours), so its vascular localization is not compromised by the leaky blood-tumor barrier.[8,20,37] Bolus administration of ferumoxytol is safe[21] and can be used sequentially with GBCA for measurement of different vascular parameters. Dual-agent dynamic imaging is quick and well tolerated in rats and humans.[8,37]

DCE-MRI is gaining wide use in the evaluation of treatment efficacy against brain tumors,[24] and for the evaluation of tumor angiogenesis.[22] Permeability measures on DCE-MRI correlate with degree of angiogenesis[23] and demonstrate the antiangiogenic effects of VEGF inhibitors[38] and sunitinib.[39] When analyzed by the "shutter speed method,"[40] the DCE-MRI time-intensity time-course data can provide measurements of K^{trans}, a rate constant for passive contrast agent plasma/interstitium transfer, and v_e, the interstitial space volume fraction (the putative contrast agent distribution volume). These tissue pharmacokinetic parameters have been validated against histopathology[41] and quantitative autoradiography.[42] In lieu of the shutter speed method, we have combined the magnitude of signal intensity changes and the time-to-peak intensity into one overall measurement of permeability.[8,37]

We have previously demonstrated that bevacizumab increased survival alone and synergistically increased the efficacy of carboplatin chemotherapy in a glioma model.[7] In the current study, bevacizumab alone decreased the rate of LX-1 tumor volume increase on both T2- and postcontrast T1-weighted MRI, whereas intetumumab actually increased tumor growth rates, although final tumor volumes were not significantly different between groups. Intetumumab has shown efficacy in preclinical studies.[13,14] A phase I clinical trial in advanced solid tumors showed intetumumab was well tolerated, and 1 of the 6 patients undergoing multiple treatments showed a prolonged tumor response.[15] In contrast, we found no tumor shrinkage in 4 different intracerebral tumor models in nude rats. The reason for the difference between our findings and published results may be the location of the tumors.

Our findings regarding changes in tumor blood volume and permeability with antiangiogenic mAbs may have clinical implications. Antiangiogenic therapy not only prevents the development of new vasculature, but it can also prune some tumor vessels and normalize the structure of others. Jain has hypothesized that these effects will normalize the tumor microenvironment, improve drug delivery, and increase the efficacy of cytotoxic therapies.[5] We show increased GBCA permeability following intetumumab but not bevacizumab. We hypothesize that normalization of brain tumor vasculature with bevacizumab restored the low-permeability characteristics of the BBB, decreasing access to GBCA and, potentially, chemotherapeutic drugs. There is some evidence that bevacizumab does not enhance chemotherapy delivery clinically, resulting in minimal if any benefit to the addition of chemotherapy to bevacizumab treatment in brain tumors.[9] In contrast to bevacizumab, intetumumab increased GBCA delivery; we hypothesize that the imaging changes will translate to increased chemotherapy delivery and therefore efficacy in brain tumor therapy. In conclusion, assessment of treatment with intetumumab in combination with chemotherapy is warranted in brain tumor clinical trials.

Acknowledgments

The authors would like to thank Sheila Taylor and Michael Pagel for their technical assistance.

Conflict of interest statement. The studies were partially funded by a sponsored research agreement from Centocor Research and Development Inc. to conduct preclinical studies of intetumumab. D.J.M. is an employee and stockholder of Centocor. The other authors have no financial interest in this agent, its developer Centocor R&D, or its parent company Johnson & Johnson.

Funding

This study was supported by a sponsored research agreement from Centocor Research and Development Inc., and NIH grants NS053468, CA137488, and NS44687 to E.A.N.

References

1. Hanahan D, Folkman J. Patterns and emerging mechanisms of the angiogenic switch during tumorigenesis. *Cell.* 1996;86:353–364.
2. Heath VL, Bicknell R. Anticancer strategies involving the vasculature. *Nat Rev Clin Oncol.* 2009;6:395–404.
3. Wong ET, Brem S. Taming glioblastoma: targeting angiogenesis. *J Clin Oncol.* 2007;25:4705–4706.
4. Ferrara N. VEGF as a therapeutic target in cancer. *Oncology.* 2005;69(suppl 3):11–16.
5. Jain RK. Antiangiogenic therapy for cancer: current and emerging concepts. *Oncology.* 2005;19:7–16.
6. Huang H, Held-Feindt J, Buhl R, Mehdorn HM, Mentlein R. Expression of VEGF and its receptors in different brain tumors. *Neurol Res.* 2005;27:371–377.
7. Jahnke K, Muldoon LL, Varallyay CG, Lewin SJ, Kraemer DF, Neuwelt EA. Bevacizumab and carboplatin increase survival and asymptomatic tumor volume in a glioma model. *Neurooncology.* 2008;11:142–150.
8. Varallyay CG, Muldoon LL, Gahramanov S, et al. Dynamic MRI using iron oxide nanoparticles to assess early vascular effects of antiangiogenic versus corticosteroid treatment in a glioma model. *J Cereb Blood Flow Metab.* 2009;29:853–860.
9. Friedman HS, Prados MD, Wen PY, et al. Bevacizumab alone and in combination with irinotecan in recurrent glioblastoma. *J Clin Oncol.* 2009;27:4733–4740.
10. Pope WB, Kim HJ, Huo J, et al. Recurrent glioblastoma multiforme: ADC histogram analysis predicts response to bevacizumab treatment. *Radiology.* 2009;252:182–189.
11. Brooks PC. Role of integrins in angiogenesis. *Eur J Cancer.* 1996;32A:2423–2429.
12. Stupack DG, Cheresh DA. Integrins and angiogenesis. *Curr Top Dev Biol.* 2004;64:207–238.
13. Chen Q, Manning CD, Millar H, et al. CNTO 95, a fully human anti alphav integrin antibody, inhibits cell signaling, migration, invasion, and spontaneous metastasis of human breast cancer cells. *Clin Exp Metastasis.* 2008;25:139–148.
14. Trikha M, Zhou Z, Nemeth JA, et al. CNTO 95, a fully human monoclonal antibody that inhibits alphav integrins, has antitumor and antiangiogenic activity in vivo. *Int J Cancer.* 2004;110:326–335.
15. Mullamitha SA, Ton NC, Parke GJM, et al. Phase I evaluation of a fully human anti av Integrin monoclonal antibody (CNTO 95) in patients with advanced solid tumors. *Clin Cancer Res.* 2007;13:2128–2135.
16. Hu LS, Baxter LC, Smith KA, et al. Relative cerebral blood volume values to differentiate high-grade glioma recurrence from posttreatment radiation effect: direct correlation between image-guided tissue histopathology and localized dynamic susceptibility-weighted contrast-enhanced perfusion MR imaging measurements. *AJNR Am J Neuroradiol.* 2009;30:552–558.
17. Law M, Young RJ, Babb JS, et al. Gliomas: predicting time to progression or survival with cerebral blood volume measurements at dynamic susceptibility-weighted contrast-enhanced perfusion MR imaging. *Radiology.* 2008;247:490–498.
18. Russell SM, Elliott R, Forshaw D, Golfinos JG, Nelson PK, Kelly PJ. Glioma vascularity correlates with reduced patient survival and increased malignancy. *Surg Neurol.* 2009;72:242–246.
19. Sadeghi N, D'Haene N, Decaestecker C, et al. Apparent diffusion coefficient and cerebral blood volume in brain gliomas: relation to tumor cell density and tumor microvessel density based on stereotactic biopsies. *AJNR Am J Neuroradiol.* 2008;29:476–482.
20. Gahramanov S, Raslan A, Muldoon LL, et al. Potential for Differentiation of Pseudoprogression from True Tumor Progression with Dynamic Susceptibility-weighted Contrast-enhanced Magnetic Resonance Imaging using Ferumoxytol vs. Gadoteridol: A Pilot Study. *J Radiation Oncol Biol Physics.* 2010; doi:10.1016/j.ijrobp.2009.10.072.
21. Weinstein J, Varallyay CG, Dosa E, et al. Superparamagnetic iron oxide nanoparticles: diagnostic magnetic resonance imaging and potential therapeutic applications in neurooncology and CNS inflammatory pathologies, a review. *J Cereb Blood Flow Metab.* 2010;30:15–35.
22. Barrett T, Brechbiel M, Bernardo M, Choyke PL. MRI of tumor angiogenesis. *J Magnetic Res Imaging.* 2007;26:235–249.
23. Veeravagu A, Hou LC, Hsu AR, et al. The temporal correlation of dynamic contrast-enhanced magnetic resonance imaging with tumor angiogenesis in a murine glioblastoma model. *Neurol Res.* 2008;30:952–959.
24. Roberts HC, Roberts TP, Brasch RC, Dillon WP. Quantitative measurement of microvascular permeability in human brain tumors achieved using dynamic contrast-enhanced MR imaging: correlation with histologic grade. *AJNR Am J Neuroradiol.* 2000;21:891–899.
25. Muldoon LL, Manninger S, Pinkston KE, Neuwelt EA. Imaging, distribution, and toxicity of superparamagnetic iron oxide magnetic resonance nanoparticles in the rat brain and intracerebral tumor. *Neurosurgery.* 2005;57:785–796.
26. Neuwelt EA, Pagel MA, Kraemer DF, Peterson DR, Muldoon LL. Bone marrow chemoprotection without compromise of chemotherapy efficacy in a rat brain tumor model. *J Pharmacol Exp Ther.* 2004;309:594–599.
27. Holash J, Maisonpierre PC, Compton D, et al. Vessel cooption, regression, and growth in tumors mediated by angiopoietins and VEGF. *Science.* 1999;284:1994–1998.
28. Soltau J, Drevs J. Mode of action and clinical impact of VEGF signaling inhibitors. *Expert Rev Anticancer Ther.* 2009;9:649–662.
29. Fiorilli P, Partridge D, Staniszewska I, et al. Integrins mediate adhesion of medulloblastoma cells to tenascin and activate pathways associated with survival and proliferation. *Lab Invest.* 2008;88:1143–1156.
30. Friedlander M, Brooks PC, Shaffer RW, Kincaid CM, Varner JA, Cheresh DA. Definition of two angiogenic pathways by distinct alphav integrins. *Science.* 1995;270:1500–1502.
31. Brooks PC, Montgomery AM, Rosenfeld M, et al. Integrin alphavbeta3 antagonists promote tumor regression by inducing apoptosis of angiogenic blood vessels. *Cell.* 1994;79:1157–1164.
32. MacDonald TJ, Taga T, Shimada H, et al. Preferential susceptibility of brain tumors to the antiangiogenic effects of an alpha(v) integrin antagonist. *Neurosurgery.* 2001;48:151–157.
33. Yamada S, Bu X-Y, Khankaldyyan V, Gonzales-Gomez I, McComb JG, Laug WE. Effect of the angiogenesis inhibitor cilengitide (EMD 121974) on glioblastoma growth in nude mice. *Neurosurgery.* 2006;59:1304–1312.
34. Reardon DA, Fink KL, Mikkelsen T, et al. Randomized phase II study of cilengitide, an integrin-targeting arginine-glycine-aspartic acid peptide, in recurrent glioblastoma multiforme. *J Clin Oncol.* 2008;26:5610–5617.
35. Kumar CC, Malkowski M, Yin Z, et al. Inhibition of angiogenesis and tumor growth by SCH221153, a dual alphavbeta3 and alphavbeta5 integrin receptor antagonist. *Cancer Res.* 2001;61:2232–2238.
36. Gutheil JC, Campbell TN, Pierce PR, et al. Targeted antiangiogenic therapy for cancer using Vitaxin: a humanized monoclonal antibody to the integrin alphavbeta3. *Clin Cancer Res.* 2000;6:3056–3061.

37. Neuwelt EA, Várallyay CG, Manninger S, et al. Potential of ferumoxytol nanoparticle MR imaging, perfusion, and angiography in CNS malignancy: a pilot study. *Neurosurgery.* 2007;60:601–611.
38. Batchelor TT, Sorensen AG, di Tomaso E, et al. AZD2171, a pan-VEGF receptor tyrosine kinase inhibitor, normalizes tumor vasculature and alleviates edema in glioblastoma patients. *Cancer Cell* 2007;11:83–95.
39. Marzola P, Degrassi A, Calderan L, et al. Early antiangiogenic activity of SU11248 evaluated in vivo by dynamic contrast-enhanced magnetic resonance imaging in an experimental model of colon carcinoma. *Clin Cancer Res.* 2005;11:5827–5832.
40. Li X, Rooney WD, Springer CS, Jr. A unified magnetic resonance imaging pharmacokinetic theory: intravascular and extracellular contrast reagents. *Magn Reson Med.* 2005;54:1351–1359.
41. Cha S, Johnson G, Wadghiri YZ, et al. Dynamic, contrast-enhanced perfusion MRI in mouse gliomas: correlation with histopathology. *Magn Reson Med.* 2003;49:848–855.
42. Ferrier MC, Sarin H, Fung SH, et al. Validation of dynamic contrast-enhanced magnetic resonance imaging-derived vascular permeability measurements using quantitative autoradiography in the RG2 rat brain tumor model. *Neoplasia.* 2007;9:546–555.